VIP Lithium-Ion Batteries Very Important Paper

Deutsche Ausgabe: DOI: 10.1002/ange.201602397
Internationale Ausgabe: DOI: 10.1002/anie.201602397

Advanced High-Voltage Aqueous Lithium-Ion Battery Enabled by "Water-in-Bisalt" Electrolyte

Liumin Suo, Oleg Borodin, Wei Sun, Xiulin Fan, Chongyin Yang, Fei Wang, Tao Gao, Zhaohui Ma, Marshall Schroeder, Arthur von Cresce, Selena M. Russell, Michel Armand, Austen Angell, Kang Xu, and Chunsheng Wang**

Abstract: *A new super-concentrated aqueous electrolyte is proposed by introducing a second lithium salt. The resultant ultra-high concentration of 28 m led to more effective formation of a protective interphase on the anode along with further suppression of water activities at both anode and cathode surfaces. The improved electrochemical stability allows the use of TiO_2 as the anode material, and a 2.5 V aqueous Li-ion cell based on $LiMn_2O_4$ and carbon-coated TiO_2 delivered the unprecedented energy density of 100 Wh kg^{-1} for rechargeable aqueous Li-ion cells, along with excellent cycling stability and high coulombic efficiency. It has been demonstrated that the introduction of a second salts into the "water-in-salt" electrolyte further pushed the energy densities of aqueous Li-ion cells closer to those of the state-of-the-art Li-ion batteries.*

Lithium-ion batteries (LIB) overwhelmingly dominate the portable electronics market (ca. 50 Wh) with their superior energy densities.[1] To withstand the high voltages (> 3.0 V) generated by the highly energetic electrochemical couples, flammable and toxic non-aqueous electrolytes have to be used, causing safety and environmental concerns that will worsen by orders of magnitude in large-scale applications, such as automotive (ca. 10^3 Wh) and grid-storage (ca. 10^6 Wh). Aqueous electrolytes that are intrinsically nonflammable and green would have provided ideal solutions. However, their narrow electrochemical stability window (1.23 V), imposed by hydrogen and oxygen evolution,[2] restricted the voltage output of such aqueous LIB under 1.50 V and resulted in severely compromised energy densities. Thus, expanding the electrochemical stability window of aqueous electrolytes becomes an issue of fundamental importance that would not only determine the practicality of aqueous LIB, but in a broader context, general aqueous electrochemistry. Unfortunately, no such effort has been reported given the significant difficulty of suppressing water decomposition reactions, in particular the reduction of water leading to hydrogen evolution, until recently when we successfully demonstrated a 3.0 V stability window when a new class of "water-in-salt" electrolyte was formulated. In such a super-concentrated electrolyte, the decomposition of salt anion occurs preferentially on the anode before hydrogen evolution occurs, leading to the formation of a dense solid electrolyte interphase (SEI) primarily consisting of LiF.[3] A 2.3 V aqueous Li-ion cell based on the electrochemical couple of $LiMn_2O_4$ and Mo_6S_8 was supported by such an electrolyte to provide an unprecedented energy density of 84 Wh kg^{-1} based on total electrode weight, which should be over 100 Wh kg^{-1} if the irreversible loss associated with SEI formation could be eliminated.[3a]

Apparently, the efficiency of forming a SEI in aqueous electrolytes depends on the salt concentration, whose increase indicates a decrease in water molecules in the solvation sphere of Li^+ and a reduction in the electrochemical activity of water. However, the high concentration (21 m; note m is molality, also called the molal concentration, not molarity) of LiTFSI (lithium bis(trifluoromethane sulfonyl)-imide) used in the "water-in-salt" electrolyte, already approaches the saturation point of this lithium salt at room temperature and corresponds to a stoichiometric compound LiTFSI $(H_2O)_{2.6}$, leaving barely any room for SEI improvement via further increase of salt concentration.[4] This situation constitutes an intrinsic barrier to maximizing the full cell energy density, as Li^+ is a limited resource therein.

It has been well-established that a hydrated salt, which could be considered a saturated electrolyte itself, could dissolve another unhydrated salt of similar chemical properties and form mixed salt systems in the molten state with higher cation/water ratios. One conspicuous example is $Ca(NO_3)_2(H_2O)_4$, which dissolves KNO_3 up to around 60 Mol %.[5] Inspired by this knowledge, we used a "water-in-salt" (WIS) electrolyte (21 m LiTFSI in water, or LiTFSI $(H_2O)_{2.6}$) as a parent hydrate salt to dissolve another lithium salt containing an anion of similar fluorinated structure, lithium trifluoromethane sulfonate (LiOTf). The mixed salt system, abbreviated "water-in-bisalt" (WIBS), consisting of 21 m LiTFSI and 7 m LiOTf provides a molten electrolyte

[*] Dr. L. Suo, W. Sun, Dr. X. Fan, Dr. C. Yang, Dr. F. Wang, T. Gao, Dr. Z. Ma, Prof. C. Wang
Department of Chemical and Biomolecular Engineering
University of Maryland
College Park, MD 20740 (USA)
E-mail: cswang@umd.edu
Dr. O. Borodin, Dr. M. Schroeder, Dr. A. von Cresce, Dr. S. M. Russell, Dr. K. Xu
Electrochemistry Branch, Sensor and Electron Devices Directorate
Power and Energy Division U.S. Army Research Laboratory
Adelphi, MD 20783 (USA)
E-mail: conrad.k.xu.civ@mail.mil
Prof. M. Armand
IC energigune, Alava Technology Park, Albert Einstein
CMIÑANO Álava (Spain)
Prof. A. Angell
School of Molecular Sciences, Arizona State University
Temp, AZ 85287 (USA)

Supporting information for this article can be found under: http://dx.doi.org/10.1002/anie.201602397.

with 28 m Li^+, or cation/water ratio of approximately 1:2. Compared with the parent "water-in-salt" system, a more compact and protective SEI is formed at higher efficiency in such highly ionic aqueous media, allowing a 2.5 V aqueous Li-ion full cell based on the electrochemical couple of $LiMn_2O_4$ and TiO_2 that delivers the highest voltage (average discharge voltage: 2.1 V) and energy density (100 Wh kg^{-1} based on the total electrode mass) amongst all aqueous battery systems to date.

Figure 1 summarizes the physicochemical properties of "water-in-bisalt" electrolytes. At room temperature, the maximum solubility of neat LiTFSI or LiOTf in H_2O is in the 21–22 m and 22–23 m, respectively, above which both salts inevitably precipitates. However, upon mixing these two salts,

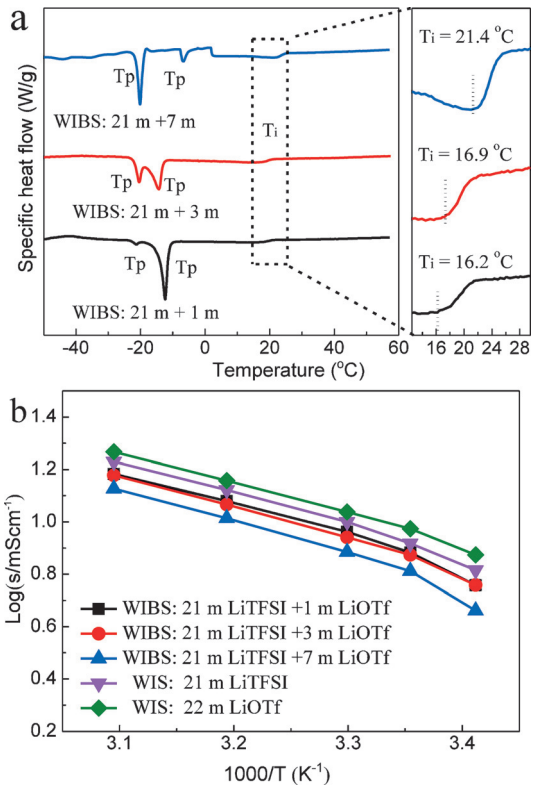

Figure 1. The physicochemical properties of the water-in-bisalt (WIBS) electrolyte (water-in-salt electrolytes: 21 m LiTFSI and 22 m LiOTf; water-in-bisalt electrolytes: 21 m LiTFSI/1 m LiOTf, 21 m LiTFSI/3 m LiOTf, and 21 m LiTFSI/7 m LiOTf). a) Thermal stability as determined by peritectic (T_p) and liquidus (T_l) temperatures measured with DSC at 1 °C min^{-1}; b) The temperature dependence of ionic conductivities in the range of −10 to around 50 °C.

the ternary system consisting of LiTFSI/LiOTf/H_2O can accommodate up to 28 m of mixed salts (21 m LiTFSI and 7 m LiOTf) at room temperature and stay liquid, despite that the Li^+/water molar ratio has now reached 0.5:1. Compared to the Li^+/water molar ratios of 0.01:1 at 1.0 m where Li^+ is coordinated by a sufficient number of water molecules, and 0.38:1 at 21 m where the shortage of water molecules in primary solvation sphere of Li^+ starts to be felt and heavy anion presence therein is expected, this unprecedented depletion of water suggests unusual behaviors, both in the bulk and interphasial. In this case, $Li(H_2O)_{2.6}^+$ in 21 m water-in-salt electrolyte can be considered as a hydrated cation that further dissolves unhydrated Li^+.[5a]

The thermal behavior for a series of such bisalt systems was characterized with differential scanning calorimetry (DSC). The liquidus temperatures of 21 m LiTFSI/7 m LiTOf starts at 21.4 °C (denoted as T_l), which is close to that of 21 m LiTFSI solution (T_l = 21.5 °C; Figure 1a and Figure S1 in the Supporting Information). Compared with the two single salt systems (21 m LiTFSI and 22 m LiOTf in H_2O), the ionic conductivities do not suffer any severe compromise, which maintain the level of 6–8 mS cm at room temperature (21 m LiTFSI + 1 m LiOTf: 7.6 mS cm, 21 m LiTFSI + 3 m LiOTf: 7.5 mS cm; and 21 m LiTFSI + 7 m LiOTf: 6.5 mS cm; Figure 1b). Closer examination of the solution structure using Raman spectra revealed that the introduction of the second salt LiOTF into the parental electrolyte 21 m LiTFSI/H_2O does not seem to induce any detectable shift of the strongest peak at 742 cm^{-1}. Since this absorption corresponds to the S-N-S bending in TFSI-structure (Figure S2), its constant position implies that the coordination environment of $TFSI^-$ is insensitive to the presence of a second anion OTf. In fact, MD simulations described in Supporting Information predicted that addition of 7 m LiOTf resulted in a displacement of about 0.5 water molecules on average from the Li^+ solvation shell by the OTf^- anion while the $Li^+/TFSI^-$ aggregation did not change significantly.

The electrochemical stability windows of WIS (21 m LiTFSI in H_2O) and WIBS (21 m LiTFSI + 7 m LiTOf in H_2O) electrolytes were evaluated with cyclic voltammetry (CV) on non-active stainless-steel mesh electrodes (Figure 2). The additional 200–300 mV shift observed in the potentials of spinel $LiMn_2O_4$ in WIBS is due to the higher lithium ion concentration in the new electrolyte, which is more concentrated than WIS by about 7 m. Figure 2b indicated that the potential for hydrogen evolution negatively shifted from 1.9 V in WIB to 1.83 V in WIBS, while the cathodic current at 1.5 V also significantly diminished from 10 mA cm^{-2} to 4 mA cm^{-2} with WIBS (Figure 2a). Meanwhile, ultrahigh Li concentration of 28 m also pushed the lithiation potential of TiO_2 and from 1.8 V to 2.0 V (Figure S3). The combined effect of the above factors should ensure that the reversible lithiation/de-lithiation of TiO_2 rests comfortably within the cathodic limits of the water-in-bisalt electrolyte. On the cathode side, the addition of 7 m LiTOf into 21 m LiTFSI did not cause any essential change in oxygen-evolution behavior (Figure 2c) as evidenced by the almost identical CV traces obtained in both electrolytes during anodic scans. Thus, the electrochemical stability window should envelop the redox potentials of the electrochemical couple $LiMn_2O_4$ and TiO_2. In fact, the CV conducted on these active electrode materials shows the characteristic redox peaks expected, that is, 4.46 V/4.30 V and 4.31 V/4.17 V for spinel $LiMn_2O_4$, and 2.36 V/1.83 V for anatase TiO_2 (Figure 2a).

An average voltage output of 2.1 V is provided by this electrochemical couple in a full Li-ion cell, which represents the highest voltage aqueous LIBs reported to date (Figure 2d). As shown in Table 1, the theoretical energy density

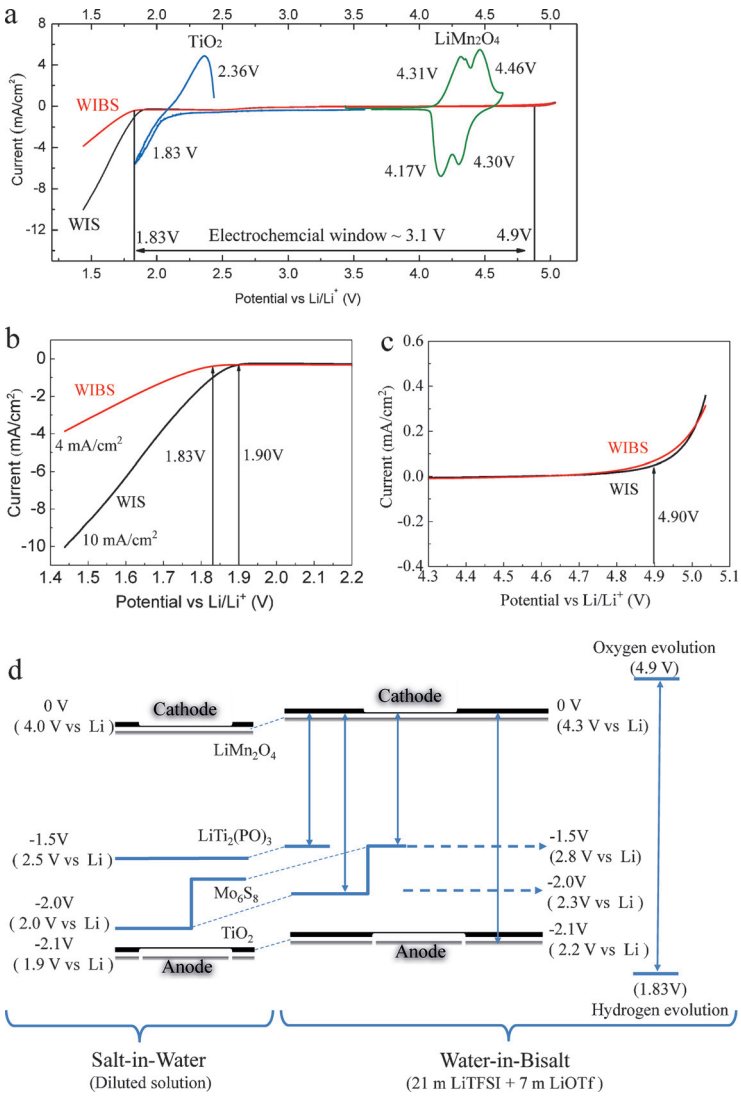

Figure 2. The cyclic voltammetry (CV) of electrolytes on different electrodes. a) the electrochemical windows of WIBS (21 m LiTFSI + 7 m LiOTf) and WIS (21 m LiTFSI) electrolyte as measured on inactive current collector (stainless-steel grid) at scanning rate of 10 mVs^{-1}, which is overlaid with the 1st CV traces collected on active anode (C-TiO_2) and cathode ($LiMn_2O_4$) materials at scanning rate of 0.1 mVs^{-1} in the same electrolyte; b) and c) the enlarged regions near anodic and cathodic extremes of the electrochemical windows on inactive current collector; d) the output voltages generated by established and our proposed electrochemical couples ($LiMn_2O_4$/$LiTiPO_4$,[6] $LiMn_2O_4$/Mo_6S_8,[3a] and $LiMn_2O_4$/TiO_2).

of such cells should reach 157 $Whkg^{-1}$ based on total electrode (cathode and anode) weight.

Given the fact that TiO_2-based materials are potent catalysts for water-splitting,[7] it is counter-intuitive to adopt it as anode material of choice in any aqueous electrolyte, as the ability to accelerate hydrogen-generation goes against the goal of stabilizing water during lithiation/de-lithiation. The high surface activity of nano-sized TiO_2 makes their application in anode materials seem even harder.[8] In addition, the intrinsic low electronic conductivity of TiO_2 also constitutes a significant barrier to the lithiation/delithiation reaction kinetics. To address these issues, a thin layer of carbon, which is highly conductive electronically but inert electrocatalytically, was applied on the TiO_2 surface via carbothermal reduction. Detailed characterizations of carbon-coated TiO_2 (hereafter denoted as C-TiO_2) are summarized in Figure S4–6 (XRD, TEM images and Raman spectra, SEM images and thermogravimetric analysis (TGA)). It seems that the TiO_2 particle morphology remains unchanged after carbon coating, while the coating is present as a rather uniform layer at the thickness of 1–2 nm, which almost makes the bulk TiO_2 invisible to the Raman. XRD further confirms that C-TiO_2 retains the pure anatase phase, while the carbon content accounts for about 12% by weight according to TGA.

The electrochemical performances of full Li-ion cells based on $LiMn_2O_4$/C-TiO_2 or $LiMn_2O_4$/TiO_2 are shown in Figure 3 and Figure S7,8. To compensate the irreversible Li consumption during SEI formation, the mass ratio of $LiMn_2O_4$ to C-TiO_2 or TiO_2 is set to be 2:1. Much higher reversible capacity of 48 $mAhg^{-1}$ and coulombic efficiency of 80.0% were obtained in the first cycle when $LiMn_2O_4$/C-TiO_2 full cell was cycled in WIBS electrolyte, as compared to the 45 $mAhg^{-1}$ and of 57.8% obtained in WIS electrolyte. An average voltage output of 2.1 V leads to an energy density above 100 $Whkg^{-1}$, which to our knowledge is the highest among all the aqueous Li-ion batteries reported. The discharge capacity slightly decreased but stabilized after 10 cycles (Figure 3b), accompanied by the coulombic efficiency approaching above 99% after 40 cycles (Figure 3d). This stabilization process indicates that the gradual formation of SEI within 40 cycles. In comparison, the same full cell in WIS electrolyte with LiTFSI as the single salt has to undergo above 60 cycles before its coulombic efficiency approaches 97%. The addition of the 7 m LiOTf in electrolyte significantly improves the cycling stability of $LiMn_2O_4$/C-TiO_2, apparently due to the more effective SEI. On the other hand, in the absence of carbon-coating, faster capacity decay was observed even when WIS electrolyte was used (Figure 3c), because on the active surfaces of the bare TiO_2 the SEI formation is seriously hindered due to substantial hydrogen evolution. It was the synergistic effects of carbon-coating on TiO_2 and the ultra-high salt concentration in water-in-bisalt electrolyte that are responsible for the excellent cycling stability for $LiMn_2O_4$/C-TiO_2 full Li-ion cell, with a low capacity decay rate of 0.22% per cycle (Figure 3c and corresponding EIS data show in Figure S8) and high coulombic efficiency of 99% after 40 cycles (Figure 3d). The excellent storage performance of full cell ($LiMn_2O_4$/WIBS/C-TiO_2) is also demonstrated by self-discharge test at 100% stage of charge (SOC; Figure S9).

A post-mortem analysis revealed the C-TiO_2 surface chemistries under varying conditions (cycle number and rate). TEM clearly imaged numerous isolated nano-sized crystalline particles (5 nm) after 10 cycles (Figure 4b–d), whose inter-

Table 1: The estimated and actual energy densities of aqueous Li-ion cells based on established and proposed electrochemical couples.

Electrochemical couples ($LiMn_2O_4$/Anode)	Theoretical capacity [Ah kg^{-1}][b]	Average discharge voltage [V]	Projected energy density [Wh kg^{-1}]	Actual energy density [Wh kg^{-1}]
$LiTi_2(PO_4)_3$	148/138	1.5	107	60 (Ref. [6])
Mo_6S_8	148/128	1.5–ca. 2.0	125	84 (Ref. [3a])
TiO_2[a]	148/150	2.1	157	100 (this work)

Note: [a] the theoretical capacity of TiO_2 is estimated on the basis of the typical discharge profile and cutoff at the end of discharge plateau not including the following slope at low potential. [b] Theoretical energy densities are calculated based on total electrode (cathode and anode) weight and the cathode and anode match by the Li molar ratio = 1:1.

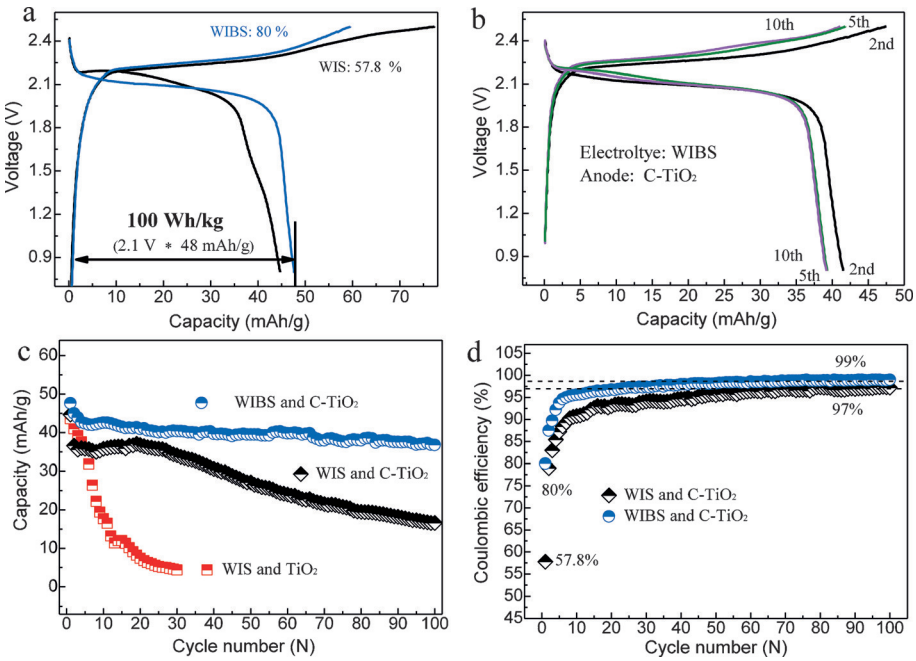

Figure 3. Electrochemical performance of full Li-ion cells based on $LiMn_2O_4$ cathode and C-TiO_2 or TiO_2 anode materials at the rate of 0.5 C (75 mA g^{-1}) between 0.8–2.5 V. a) The first charge–discharge profiles of the electrochemical couples of $LiMn_2O_4$/C-TiO_2 in WIS (black) and WIBS (blue); the Coulombic efficiencies are labeled in the graph; b) The charge–discharge profiles of the electrochemical couple of $LiMn_2O_4$/C-TiO_2 in WIBS at the 2nd, 5th, and 100th cycles, c) and d) The cycling stability and Coulombic efficiencies for varying combinations of TiO_2 anode and electrolyte.

planar space is about 0.198 nm, far larger than the (101) interplanar spacing of anatase TiO_2 (0.351 nm) but rather close to (200) interplanar spacing of LiF (0.204 nm). XPS also detected additional F1s signal at 684.67 eV in both 21 m LiTFSI + 7 m LiOTf and 22 m LiOTf that corresponds to LiF on cycled C-TiO_2 (Figure 4 g and Figure S10), which is absent on the pristine C-TiO_2 surface that was only exposed to the electrolyte (Figure 4 f). Both TEM and XPS directly confirm the presence of an interphase that primarily consists of LiF, which originates not only from LiTFSI but also from LiOTf-reduction as predicted by quantum chemistry (QC) calculations described below. Since the SEI has not been formed completely owing to the limited cycling (10 cycles), the LiF abundance is not as conspicuous as compared with our earlier results,[3a] but high-resolution TEM images of the C-TiO_2 surface after prolonged cycling indicated the time dependence of SEI growth (Figure 4 e), where, after 143 cycles, C-TiO_2 was entirely covered by a large amount of nano-LiF particles that would constitute a uniform SEI of 5–10 nm thick.

Quantum chemical calculations shown in Figure 5 indicate that the LiOTf contact ion pairs have reduction potential below that of hydrogen evolution, while the ionic aggregates, in which the anions are coordinated by multiple Li^+, have reduction potentials above that of hydrogen evolution, yielding LiF as the reduction product. The reorganization energies for the LiOTf and LiTFSI aggregates during reduction and LiF formation were also found to be similar indicating that both salts are likely to contribute to SEI formation at approximately the same rate (Figure S11). MD simulations predicted that most anions in the bisalt electrolyte are coordinated by two or three Li + cations supporting the choice of model compounds for QC calculations. Moreover, addition of 7 m LiOTf to 21 m LiTFSI solution not only displaced around 0.5 waters per Li^+ solvation shell but also reduced the fraction of free water from 0.15 to 0.11. "Free water" refers to water molecules that remain uncoordinated by any Li^+ ions. A diminished fraction of free water further contributes to the enhanced redox stability of electrolyte.

Based on the above observations, we conclude that the unprecedented high cell voltage (2.5 V), energy density (100 Wh/Kg) and excellent cycling stability are achieved in an aqueous full Li-ion cell based on the electrochemical couple of $LiMn_2O_4$ and C-TiO_2 via deactivation of the catalytic surface of nano-sized TiO_2 with carbon-coating and super-concentrated aqueous electrolyte with salt-mixing. The catalytically inert carbon effectively introduced an extra kinetic barrier to water splitting, while its high electron conductivity significantly reduces charge transfer resistance as well as ohmic polarization. On the other hand, the ultra-high salt concentration in the new bisalt electrolyte makes it easier for the salt anion to be reduced, thus providing the opportunity to form a more protective SEI before hydrogen evolution. Additional benefits of the super-concentrated aqueous electrolyte also include the further reduction in electrochemical activity of water, while depressing the

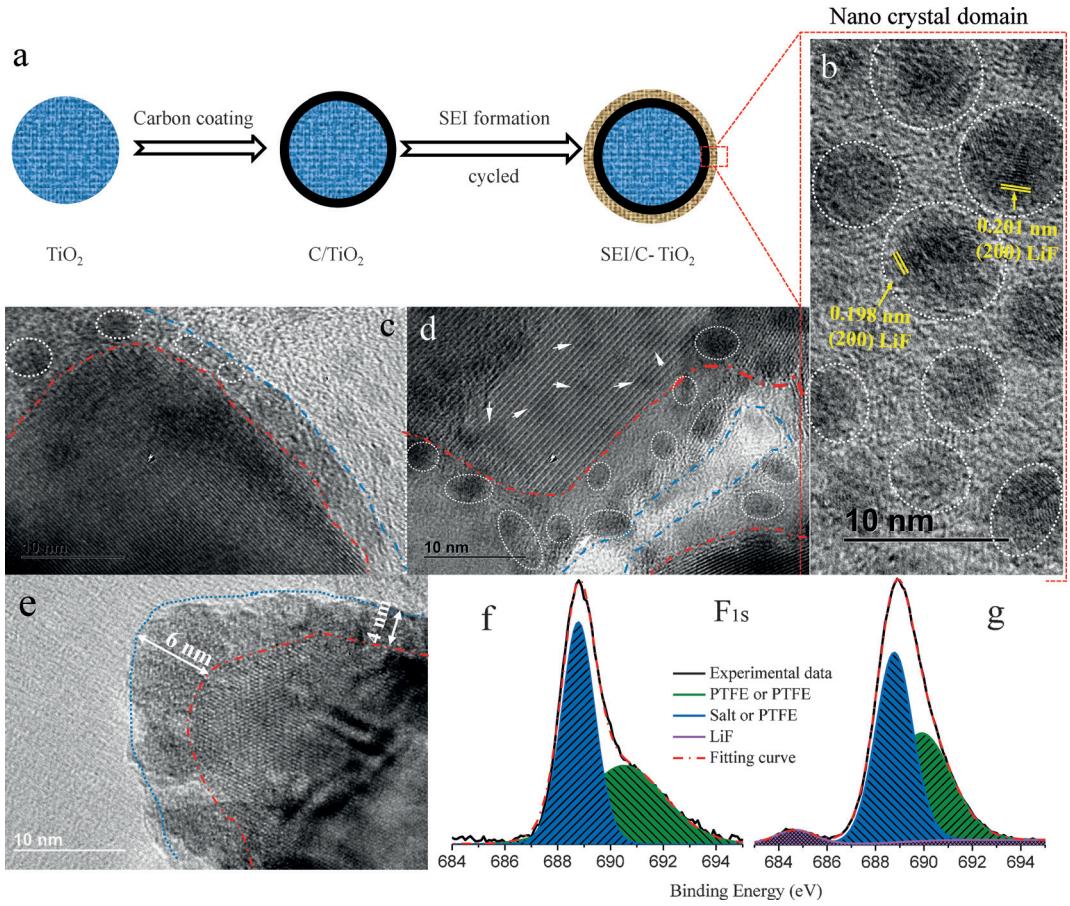

Figure 4. Post-mortem analysis on the cycled anatase C/TiO_2 in water-in-bisalt electrolyte. a) the schematic illustration of TiO_2 surface pre-coated by carbon and in situ coated by SEI, b)–d) TEM images of C-TiO_2 recovered after 10 cycles at 0.5 C; and e) after 143 cycles at 1 C. Red and blue broken lines denoted outer and inner edge of SEI layer, white arrows and dotted circles marked the crystal domain of SEI in anode surface; f) and g) X-ray photoelectron spectroscopy (XPS) of C-TiO_2 electrode before and after 10 cycles at 0.5 C, respectively.

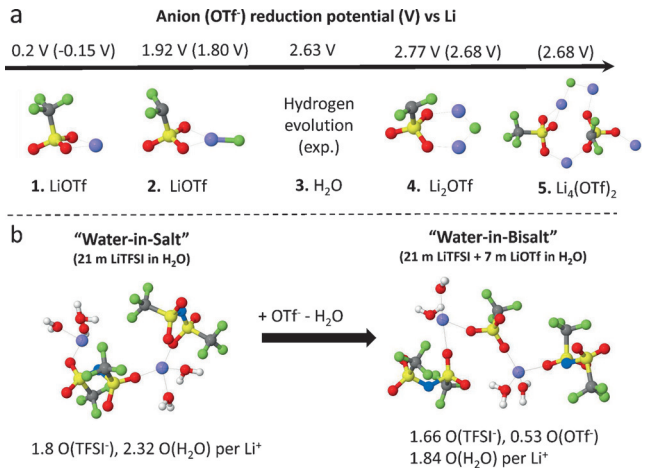

Figure 5. a) Reduction stability of LiOTf complexes versus Li/Li^+ from G4MP2 and M05-2X/6-31 + G(d,p) (in parentheses) QC calculations with surrounding water represented using a water implicit solvent model; b) a schematic representation of the influence of addition of 7 m LiOTf on the solvate structure and the composition of the Li^+ first coordination shell extracted from MD simulations with the focus on oxygen atoms (purple Li, red O, green F, yellow S, gray C, white H and blue N).

liquidus temperature of the electrolyte. Such improvements enabled our continued efforts of pushing the energy densities of aqueous Li-ion cells to a level closer to those of the state-of-the-art LIB, while keeping the cells absolutely nonflammable.

In summary, we proposed a new class of electrolyte termed a "water-in-bisalt" (WIBS) electrolyte with a wider electrochemical stability window and lower water activity. The unprecedented high ionic density in the solution effectively suppresses hydrogen evolution and promotes the formation of a more protective SEI. A full Li-ion cell based on $LiMn_2O_4$ and C-TiO_2 is demonstrated in such an electrolyte, which delivered the highest average discharge voltage (2.1 V) and energy density (100 $Wh\,kg^{-1}$) among all rechargeable aqueous Li-ion batteries reported thus far. The introduction of a second or even more salts into the water-in-salt electrolyte could pave the pathway to more energetic aqueous Li-ion batteries with energy densities competitive against the state-of-the-art lithium-ion batteries.

Acknowledgements

C.W. and K.X. gratefully acknowledge funding from DOE ARPA-E (DEAR0000389). We also thank the support of the Maryland Nano Center and its Nisp Lab and SAC Lab, and Dr. Karen Gaskell for their technical support and helpful discussion. Modeling efforts were supported by ARL Enterprise for Multiscale Research of Materials.

Keywords: anatase TiO_2 · aqueous batteries · electrolyte · lithium-ion batteries · water-in-bisalt

How to cite: *Angew. Chem. Int. Ed.* **2016**, *55*, 7136–7141
Angew. Chem. **2016**, *128*, 7252–7257

[1] a) K. Xu, *Chem. Rev.* **2004**, *104*, 4303–4417; b) J. B. Goodenough, Y. Kim, *Chem. Mater.* **2010**, *22*, 587–603; c) K. Xu, *Chem. Rev.* **2014**, *114*, 11503–11618; d) L. Suo, Y.-S. Hu, H. Li, M. Armand, L. Chen, *Nat. Commun.* **2013**, *4*, 1481.

[2] a) H. Kim, J. Hong, K.-Y. Park, H. Kim, S.-W. Kim, K. Kang, *Chem. Rev.* **2014**, *114*, 11788–11827; b) Y. Wang, J. Yi, Y. Xia, *Adv. Energy Mater.* **2012**, *2*, 830–840; c) W. Li, J. R. Dahn, D. S. Wainwright, *Science* **1994**, *264*, 1115–1118; d) J.-Y. Luo, W.-J. Cui, P. He, Y.-Y. Xia, *Nat. Chem.* **2010**, *2*, 760–765; e) C. Wessells, R. A. Huggins, Y. Cui, *J. Power Sources* **2011**, *196*, 2884–2888.

[3] a) L. Suo, O. Borodin, T. Gao, M. Olguin, J. Ho, X. Fan, C. Luo, C. Wang, K. Xu, *Science* **2015**, *350*, 938–943; b) L. Suo, F. Han, X. Fan, H. Liu, K. Xu, C. Wang, *J. Mater. Chem. A* **2016**, DOI: 10.1039/C6TA00451B.

[4] a) E. Peled, *J. Electrochem. Soc.* **1979**, *126*, 2047–2051; b) A. J. Smith, J. C. Burns, X. Zhao, D. Xiong, J. R. Dahn, *J. Electrochem. Soc.* **2011**, *158*, A447–A452.

[5] a) C. A. Angell, *J. Electrochem. Soc.* **1965**, *112*, 1224–1227; b) C. A. Angell, N. Byrne, J.-P. Belieres, *Acc. Chem. Res.* **2007**, *40*, 1228–1236.

[6] J.-Y. Luo, Y.-Y. Xia, *Adv. Funct. Mater.* **2007**, *17*, 3877–3884.

[7] a) A. Fujishima, X. T. Zhang, D. A. Tryk, *Surf. Sci. Rep.* **2008**, *63*, 515–582; b) S. U. M. Khan, M. Al-Shahry, W. B. Ingler, *Science* **2002**, *297*, 2243–2245; c) M. Ni, M. K. H. Leung, D. Y. C. Leung, K. Sumathy, *Renewable Sustainable Energy Rev.* **2007**, *11*, 401–425.

[8] a) J. Rossmeisl, Z. W. Qu, H. Zhu, G. J. Kroes, J. K. Norskov, *J. Electroanal. Chem.* **2007**, *607*, 83–89; b) H. J. Kim, D. H. K. Jackson, J. Lee, Y. Guan, T. F. Kuech, G. W. Huber, *ACS Catal.* **2015**, *5*, 3463–3469; c) C. G. Morales-Guio, L.-A. Stern, X. Hu, *Chem. Soc. Rev.* **2014**, *43*, 6555–6569.

Received: March 9, 2016
Published online: April 27, 2016

